

Optimized Channel Geometry of a Flow-Focusing Droplet Generator for Parallelization.

D. Conchouso*, E. Rawashdeh, D. Castro, A. Arevalo, I. G. Foulds
King Abdullah University of Science and Technology
4700 KAUST 23955, david.conchouso@kaust.edu.sa

Abstract: This document presents the Computational Fluid Dynamics (CFD) simulation of a commonly used Microfluidic Droplet Generator (MFDG) using the Laminar Two-Phase Flow, Phase Field method in COMSOL Multiphysics®. The paper discusses the effect of the channel's geometry in droplet size and proposes a guide to best select a cross-sectional area with low droplet size dynamic range that could be advantageous for massive parallelization of microfluidic droplet generators.

Keywords: droplet generator, microfluidics, water in oil droplets, COMSOL, parallelization.

1. Introduction

Microfluidics is a continuously growing research area that has shown promising results to revolutionize the standard and quality of human living. The micro-world, in which these fluidic systems exist, offers great scaling advantages over common macro-scale devices, such as chemical reactors, cell and tissue growth and study, disease diagnostic [1], [2]. In this scale, surface forces are vastly more significant than body forces since they scale quadratically with the length while volume-related phenomena scale cubically. This fact can be used to design systems with faster dynamic response, smaller footprint, higher sensitivity, and cheaper cost for point-of-care and lab-on-chip applications. Another important consideration of microfluidic systems is the fact that due to their scale, their flow behavior is laminar.

Within the microfluidic context, droplet-based microfluidics make use of small volumes (droplets) of fluids to carry out different chemical reactions and assays[2]-[4]. The devices that are used to create these droplets are called Microfluidic Droplet Generators (MFDG). MFDGs produce monodisperse emulsions of two immiscible fluids when shearing forces of a continuous phase (CP) overcome the surface tension of the disperse phase (DP), thus forming droplets. These oil-in-water O/W or water-in-oil

W/O droplets, are then used as confined reaction containers in which reagents and conditions can be manipulated to our benefit. Since these droplets are in the order of Pico-liter to Nano-liter volumes the reagent consumption is minimal thus allowing high-throughput screening of chemical libraries and conditions at low cost, and offering a unique environment for chemical synthesis.

Applications of this technology are found in high added value industries such as those in pharmaceuticals, photonics, aggressive chemical industry, small molecule synthesis, molecular biology, and cosmetics [1]-[6].

Droplet generators with various geometries and characteristics have been summarized in various review papers [3], [7], [8]. The microfluidic droplet generator simulated in this paper is a very popular device within the microfluidic community also known as a 2D flow focusing droplet generator. This MFDG consists of a cross shaped constriction that focuses the disperse phase into a long thread prior to droplet formation. Due to this characteristic, it is possible to generate droplets with different sizes. Droplet size in this type of microfluidic devices depends on several parameters such as: the dynamic behavior related to the flow rates, intrinsic properties of the fluids (viscosities, densities and interfacial tension) and parameters correspondent to the geometry of the device. In this paper we will study this last parameter in order to find a suitable geometry for parallelization[9].

Since the output volume of a single MFDG is low, parallelizing several of these devices is a natural solution to meet the demands of industrial-scale production. Although this is a simple idea, its practical realization is not trivial. Crosstalk between parallel channels due to coupled pressure changes in the fluids affects the aggregated output's monodispersity. To minimize this problem, a solution we propose is finding geometry with low sensitivity to flow rate changes and can operate adequately despite flow rate variations.

In order to understand the channel shape's effect on the droplet generation, the droplet size output of several devices with different constriction channel geometries (same hydraulic diameter) at the same flow rates will be compared. This will allow us find an optimized shape to design a droplet generator with low droplet size dynamic range for parallelization.

Moreover, by simulating in a three dimensional space, we also learn about the effect of a height difference (deeper channel) at the exit of the constriction in the dynamics of the system

1.1 Importance for Computational Fluid Dynamic (CFD) simulations

The fabrication, operation and testing of a microfluidic droplet generator is a challenging and time consuming task that requires specialized equipment. Characterization of droplets is typically done by post-processing images taken with high-speed cameras. For these reasons, it is advantageous to perform a few design iterations aided by a computational fluid dynamic simulation prior to actual fabrication. Additionally, fabrication defects, particularly in the constriction (channel section where the droplets are formed), can have a large impact on the device's performance, and previous simulation can provide a baseline to compare individual devices.

2. Two-Dimensional Flow-Focusing Droplet Generator Devices

The MFDG proposed here (Figure 1) is a cross-shape microstructure in which two microfluidic channels of similar geometry intersect in a point to create a localized constriction. This intersection brings together both liquid phases and promotes the droplet formation. This device is known as a flow focusing droplet generator because the *CP* focuses laterally a stream of *DP*. This bidirectional focusing elongates the DP and due to the shear forces a droplet breaks off in a repeatable and reliable fashion. Our flow-focusing constriction is connected with a deeper output channel (400um-deep channel) at the output of the generator in order to expand the capillary number range in which droplets are formed[10].

Three different cross-sectional areas with the same hydraulic diameter ($D_h = 100\mu\text{m}$) were evaluated in this simulation (Figure 1). The dimensions of these cross-sectional areas were selected in such a way that they can be fabricated in Poly (methyl-methacrylate) PMMA using a milling machine and the commercially available RF end-mills and micro-cutters from LPKF PCB routers. Two rectangular areas with dimensions of $285 \times 61\mu\text{m}$ and $150 \times 75\mu\text{m}$ were simulated. By varying the width and height of these rectangles we can study the walls effects during the droplet formation. Finally the third area is a $200 \times 100\mu\text{m}$ trapezoid with $50\mu\text{m}$ -wide minor base.

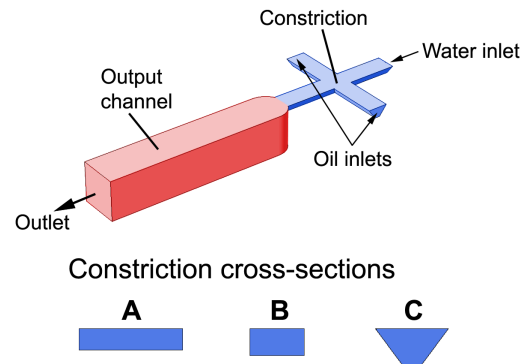


Figure 1. Flow-Focusing Microfluidic Droplet Generator Diagram. The device is comprised of a cross-shape constriction with different cross-sectional areas and a wider and deeper output channel ($400 \times 400\mu\text{m}$). A) Rectangular $285 \times 61\mu\text{m}$, B) Rectangular $150 \times 75\mu\text{m}$, and C) $200 \times 100\mu\text{m}$ trapezoid with $50\mu\text{m}$ -wide minor base.

3. Laminar Two-Phase Flow, Phase Field Model

Laminar flow is the typical flow regimen for these microfluidic droplet generators since the Reynolds number, relating inertia and viscous forces, scales proportional to the length and therefore becomes very small in the micro-scale.

$$Re = \frac{\rho u L}{\mu}$$

Where u is the velocity (m/s), μ is the dynamic viscosity (Pa s), ρ is the density (Kg/m^3) and L is the characteristic length (m).

The phase field method was selected among other models because it can give a continuous tracking of the fluid interface using an energy model that can later be coupled with other

physics such as diffusion and heat transfer for a more complex simulation. The Laminar two-phase flow, Phase Field physics module was used to model the flow-focusing device in three and two-dimensional spaces. A detailed description of this method can be found elsewhere [11].

In the phase field method, the multiphase flow is described with the help of a variable known as the *order parameter* represented by the Greek letter ϕ . The disperse phase is defined as the fluid element in which $\phi = 1$, the surrounding media (i.e. continuous phase) is represented by $\phi = 0$. Finally, the set of values $1 < \phi < 0$ represents the interface between both phases, also known as the phase field.

The phase field module on COMSOL Multiphysics® uses the incompressible formulation of the Navier-Stokes equations to describe the fluid evolution in the multiphase system. The Navier-Stokes general equation for conservation of momentum is solved for default in the module:

$$\rho \left(\frac{\partial \mathbf{u}}{\partial t} + (\mathbf{u} \cdot \nabla) \mathbf{u} \right) = \nabla \cdot [-p\mathbf{I} + \mu(\nabla \mathbf{u} + \nabla \mathbf{u}^T)] + \mathbf{F}_g + \mathbf{F}_{st} + \mathbf{F}$$

Where \mathbf{u} is the velocity vector, p is the pressure, μ is the dynamic viscosity, ρ is the density of the fluid element, and \mathbf{F} are all the external forces affecting the motion. The simulation also considers the continuity equation in order to satisfy the condition of conservation of mass for the incompressible flow:

$$\nabla \cdot \mathbf{u} = 0$$

For the interface tracking the phase field method defines two tracking parameters, represented by the Greek characters λ, ε . The first one is the mixing energy density and the second one, also known as capillary width ε , is related with the interface thickness. These two parameters are related by means of the surface tension in this simulation:

$$\sigma = \frac{2\lambda(2)^{1/2}}{3\varepsilon}$$

In order to fully describe the behavior of the flow, COMSOL Multiphysics® uses those parameters to make the following relations:

$$\frac{\partial \phi}{\partial t} + \mathbf{u} \cdot \nabla \phi = \nabla \cdot \frac{\gamma^\lambda}{\varepsilon} \nabla \psi$$

$$\psi = -\nabla \cdot \varepsilon^2 \nabla \phi + (\phi^2 - 1)\phi + \left(\frac{\varepsilon^2}{\lambda} \right) \frac{\partial f_{ext}}{\partial \phi}$$

4. Simulation Setup

In this paper, we have simulated a MFDG in a two dimensional space which has given us information about expected flow rates and boundary conditions for a more complex simulation in a three dimensional environment. However, these 2D simulations lack information relative to the step increment from the output channel and therefore a three-dimensional simulation is closer to reality.

For all these simulations, only half of the device was drawn to simplify the number of nodes and operations by using the symmetry boundary condition. Cross-sections of the device were drawn in in Autodesk® AutoCAD and imported into COMSOL, which were then extruded to the correct dimensions. We selected a physics-controlled mesh with free tetrahedral geometry, with extra coarse element size.

We used an iterative GMRES solver for the phase initialization and a direct PARDISO solver for the time-dependent study. The time range was typically between 0 and 0.5 s, with step increments of 0.02 s.

Although oil in water O/W and water in oil W/O droplets are achievable using structures similar to this one, in this paper we will only focus on the W/O droplet case since the wetting conditions of PMMA are favorable for this chemistry. The surfaces indicated in Figure 1 were defined as port inlets for water and oil, with a fixed flow rate. The outlet was set as 0 pressure with no viscous stress. The continuous phase used is light mineral oil (Sigma Aldrich, CAS: 8042-47-5), with $\rho = 0.838 \text{ g/cm}^3$, $\nu = 14.2 \text{ cst}$. The surface tension between oil and water used was $\sigma = 50 \text{ mN/m}$ [12].

The simulations were executed with a wetted wall condition using a contact angle of 135 degrees. This parameter was measured using a goniometer KRUSS DSA100W drop shape

analysis system. A water droplet placed on a Polymethyl methacrylate (PMMA) substrate immersed in mineral oil was photographed (Figure 2), the contact angle is measured from this picture.

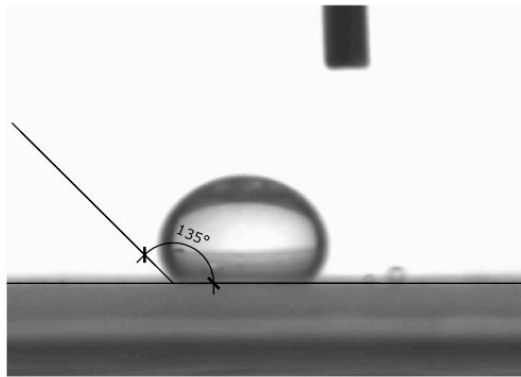


Figure 2. Static contact angle measurement using sessile drop method. Deionized water droplet on PMMA substrate, surrounded by mineral oil, contact angle = 135 degrees.

5. Simulation Results

Using the post processing tools, we were able to create graphics that display the volume fraction of water in oil isosurfaces, velocity field streamlines of flow, and velocity magnitude at the axis of symmetry (Figure 3).

The streamlines show a predominantly laminar flow in the channels, however at larger flow rates, stable current vortices appear at the height change where the constriction meets the output channel.

The velocity magnitude along the plane of symmetry is higher at the constriction, promoting the focusing behavior of the device

To obtain the effective droplet diameter (D_{eff}) we performed a volume integration of the volume fraction of water along a section of the output channel, and calculate it according to:

$$D_{eff} = 2 \cdot \sqrt[3]{\frac{3}{4\pi} \cdot V_{droplet}}$$

Using this model we evaluated the effective droplet diameter for two total flow rates with different water and oil flow rate ratios. The two selected total flows were 300 $\mu\text{l}/\text{min}$ and 30 $\mu\text{l}/\text{min}$; and the flow rate ratios were 1:1, 1:1.5, 1:2, 1:3 and 1:5.

The droplet size versus the flow rate ratio is shown in Figure 4. The droplet size dynamic range is shown in Table 1.

Table 1. Droplet Size Dynamic Range for the three different cross-sectional areas evaluated.

Cross-sections	Dimensions (μm)	ΔD_{eff} @ 300 ($\mu\text{l}/\text{min}$)	ΔD_{eff} @ 30 ($\mu\text{l}/\text{min}$)
A	285x61	1.10	1.67
B	150x75	2.33	2.35
C	200x100, 50	2.12	2.59

The droplet size dynamic range for the wide rectangular cross-section (285x61 μm) was smaller for both total flow rates. Therefore, this generator geometry works best for parallelization.

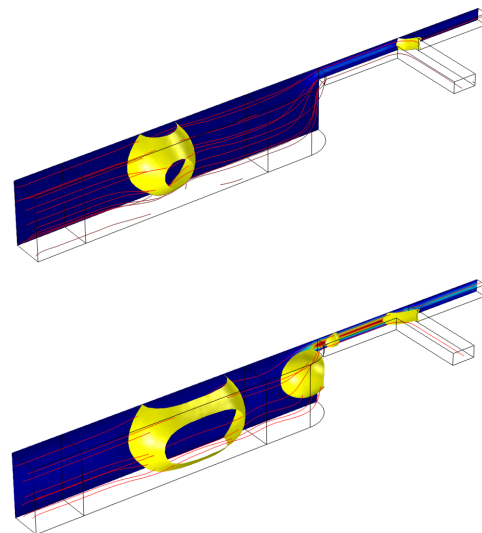


Figure 3. CFD simulation of the MFDG, with symmetry boundary condition. Top: Oil flow rate = 22.5 $\mu\text{l}/\text{min}$ and water flow rate = 7.5 $\mu\text{l}/\text{min}$, droplet effective diameter = 450 μm . Bottom: Oil flow rate = 18 $\mu\text{l}/\text{min}$ and water flow rate = 12 $\mu\text{l}/\text{min}$, droplet effective diameter = 550 μm .

6. Conclusions

This paper presents a study of the behavior of a common two-dimensional flow-focusing droplet generator at different flow rates and flow rate ratios for the production of water-in-oil emulsions. The study evaluates three different channel geometries for a cross-shape constriction

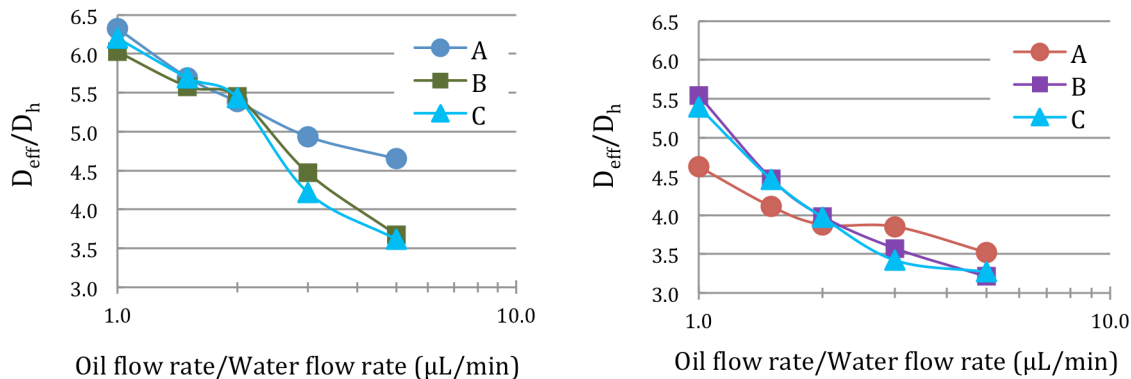


Figure 4. Plots of effective droplet diameter normalized to the channels hydraulic diameter ($D_h=100\ \mu\text{m}$) versus oil and water flow rate ratio at a constant flow rate. Left: Total flow rate = $30\ \mu\text{L}/\text{min}$, and Right: Total flow rate = $300\ \mu\text{L}/\text{min}$. A: Rectangular cross-section $285\times 61\ \mu\text{m}$, B: Rectangular cross-section $150\times 75\ \mu\text{m}$, C: Trapezoidal cross-section $200\times 100\ \mu\text{m}$, with $50\ \mu\text{m}$ minor base.

to help determine an optimal geometry of an easily manufacturable MFDG for parallelization. The wide and shallow rectangular geometry is preferable over the other geometries evaluated (i.e. narrower rectangular and trapezoidal geometries) since it showed the lowest variability in droplet size with changing water/oil flow rate ratio. This trend was present in both studies performed at different total flow rates, making the shallow rectangular geometry the most adequate for parallelization.

At high total flows (i.e. $300\ \mu\text{L}/\text{min}$), larger capillary number, this behavior is more pronounced than at low flows (i.e. $30\ \mu\text{L}/\text{min}$). This behavior could be due to the reduced influence of the sidewalls in the generator.

7. References

1. G. M. Whitesides, "The origins and the future of microfluidics," *Nature*, **vol. 442**, pp. 368–373, (2006).
2. H. Song, D. L. Chen, and R. F. Ismagilov, "Reactions in Droplets in Microfluidic Channels," *Small*, **vol. 45**, pp. 7336–7356, (2006).
3. J.-T. Wang, J. Wang, and J.-J. Han, "Fabrication of Advanced Particles and Particle-Based Materials Assisted by Droplet-Based Microfluidics," *Small*, **vol. 7**, pp. 1728–1754, (2011).
4. A. B. Theberge, F. courtois, Y. schaeerli, M. Fischlechner, C. Abell, F. Hollfelder, and W. T. S. Huck, "Microdroplets in Microfluidics: An Evolving Platform for Discoveries in Chemistry and Biology," *Small*, **vol. 49**, pp. 5846–5868 (2010).
5. S.-Y. Teh, R. Lin, L.-H. Hung, and A. P. Lee, "Droplet microfluidics," *Lab on a Chip*, **vol. 8**, p. 198, (2008).
6. J. I. Park, A. Saffari, S. Kumar, A. Günther, and E. Kumacheva, "Microfluidic Synthesis of Polymer and Inorganic Particulate Materials," *Annu. Rev. Mater. Res.*, **vol. 40**, pp. 415–443, (2010).
7. G. T. Vladislavjević, I. Kobayashi, and M. Nakajima, "Production of uniform droplets using membrane, microchannel and microfluidic emulsification devices," *Microfluid Nanofluid*, **vol. 13**, pp. 151–178, (2012)
8. G. F. Christopher and S. L. Anna, "Microfluidic methods for generating continuous droplet streams," *J. Phys. D: Appl. Phys.*, **vol. 40**, pp. R319–R336, (2007).
9. C. Holtze, "Large-scale droplet production in microfluidic devices—an industrial perspective," *J. Phys. D: Appl. Phys.*, **vol. 46**, p. 114008, (2013).
10. Chan, A. Alivisatos, and R. Mathies, "High-temperature microfluidic synthesis of CdSe nanocrystals in nanoliter droplets," *J Am Chem Soc*, **vol. 127**, pp. 13854–13861, (2005).

11. P. Yue, J. J. Feng, C. Liu, and J. Shen, "A diffuse-interface method for simulating two-phase flows of complex fluids," *Journal of Fluid Mechanics*, (2004).
12. C. A. Stan, S. K. Y. Tang, and G. M. Whitesides, "Independent Control of Drop Size and Velocity in Microfluidic Flow-Focusing Generators Using Variable Temperature and Flow Rate," *Anal. Chem.*, **vol. 81**, pp. 2399–2402, (2009).